Pergamon

0038-1101(95)00023-2

Solid-State Electronics Vol. 38, No. 11, pp. 1945–1952, 1995
Copyright © 1995 Elsevier Science Ltd
Printed in Great Britain. All rights reserved
0038-1101/95 $9.50 + 0.00

AN EXPLICIT PHYSICAL MODEL FOR THE LONG-CHANNEL MOS TRANSISTOR INCLUDING SMALL-SIGNAL PARAMETERS

ANA ISABELA ARAÚJO CUNHA,† MÁRCIO CHEREM SCHNEIDER and CARLOS GALUP-MONTORO

Departamento de Engenharia Elétrica, Universidade Federal de Santa Catarina, C.P. 476, CEP 88040-900, Florianópolis, SC, Brazil

(Received 3 May 1994; in revised form 27 January 1995)

Abstract—This paper presents a long-channel MOSFET model wherein the drain current, total charges and small-signal parameters for quasi-static operation are very simple functions of the inversion charge densities at the channel boundaries. The inversion charge densities, in turn, are formulated as explicit continuous functions of the terminal voltages, with continuous first order derivatives, resulting in an explicit MOSFET model valid in the whole inversion region. Physical properties, such as the symmetry of the transistor with respect to source and drain are carefully observed in order to achieve a proper prediction of the device behavior. The proposed model contains only the classical parameters of the MOSFET theory.

NOTATION

A auxiliary parameter (m^2)
B auxiliary parameter ($m^4/(Cs)$)
C_{bd} bulk–drain capacitance (F)
C_{bs} bulk–source capacitance (F)
C_{gb} gate–bulk capacitance (F)
C_{gs} gate–source capacitance (F)
C_{gd} gate–drain capacitance (F)
C_{ox} oxide capacitance (F)
C'_b depletion capacitance per unit area (F/m^2)
C'_c semiconductor capacitance per unit area (F/m^2)
C'_g gate capacitance per unit area (F/m^2)
C'_i inversion capacitance per unit area (F/m^2)
C'_{ox} oxide capacitance per unit area (F/m^2)
g_{mD} drain transconductance (S)
g_{mG} gate transconductance (S)
g_{mS} source transconductance (S)
I_D drain current (A)
L effective channel length (m)
n slope factor (dimensionless)
N_A acceptor concentration (m^{-3})
Q_B total depletion charge (C)
Q_G total gate charge (C)
Q_I total inversion charge (C)
Q_0 effective interface charge (C)
Q'_B depletion charge density (C/m^2)
Q'_C semiconductor charge density (C/m^2)
Q'_F shifted inversion charge density at source (C/m^2)
Q'_I inversion charge density (C/m^2)
Q'_{ID} inversion charge density at drain (C/m^2)
Q'_{IS} inversion charge density at source (C/m^2)
Q'_{It} shifted inversion charge density (C/m^2)
Q'_R shifted inversion charge density at drain (C/m^2)
t_{ox} oxide thickness (m)
V_B bulk voltage (V)
V_{CB} channel voltage = difference between the electron quasi-Fermi potential and the bulk Fermi potential (V)
V_D drain voltage (V)
V_{DB} drain-to-bulk voltage (V)
V_{DS} drain-to-source voltage (V)
V_{FB} flat-band voltage (V)
V_G gate voltage (V)
V_{GB} gate-to-bulk voltage (V)
V_{GS} gate-to-source voltage (V)
V_P "pinch-off" voltage (V)
V_S source voltage (V)
V_{SB} source-to-bulk voltage (V)
V_{T0} threshold voltage at equilibrium (V)
W effective channel width (m)
γ body effect factor ($V^{0.5}$)
ϕ_F Fermi potential of bulk (V)
ϕ_S surface potential (V)
ϕ_{SL} surface potential at drain (V)
ϕ_{S0} surface potential at source (V)
ϕ_t thermal voltage (V)
μ carrier mobility ($m^2/(V\ s)$)

1. INTRODUCTION

MOSFET models included in circuit simulators are based on either the regional approach[1–3], or surface potential formulations[5–9] or semiempirical equations[10–14]. Models based on the regional approach[1–3] use different sets of equations to describe the device behavior in different regions of device operation. In this traditional modeling approach, the weak and strong inversion regions are generally bridged by using a non-physical curve fitting. However, this procedure often causes large errors or discontinuities in the small-signal parameters such as conductances and capacitances. This

†Permanent address: Departamento de Engenharia Elétrica da Escola Politécnica, Universidade Federal da Bahia, CEP 40210-630, Salvador, BA, Brazil.

results in a model that is inaccurate for analog applications[4], where the MOSFET operates frequently in the moderate inversion region. Moreover, the discontinuity in a.c. parameters can lead to numerical oscillations. Models based on surface potential formulations are inherently continuous; however, they demand the solution of an implicit equation for the surface potential, often resulting in significant computing time penalty. Finally, semiempirical MOSFET models generally take the risk of becoming neither scalable nor suited for statistical analysis owing to the introduction of empirical parameters.

This paper presents an explicit model of the long-channel MOS transistor valid in all regions of operation. The drain current, the total charges and the small-signal parameters are expressed as very simple functions of the inversion charge densities at the source and drain ends. An approximation of the semiconductor capacitance[15] allows determining explicit expressions for the inversion charge density in terms of the terminal voltages. As a consequence, the MOSFET static and dynamic characteristics have an explicit formulation in terms of the terminal voltages.

2. APPROXIMATION OF THE CHARGE DENSITIES

The expressions and discussions that follow are related to the long channel nMOS transistor, illustrated in Fig. 1. Uniform substrate doping and field-independent mobility have been assumed in our analysis. According to the equation of potential balance in the MOS structure, in the inversion region of operation[1, p. 79]:

$$V_{GB} - V_{FB} = \phi_S + \gamma\sqrt{\phi_S + \phi_t\, e^{(\phi_S - 2\phi_F - V_{CB})/\phi_t}} \quad (1)$$

where ϕ_S is the surface potential and $\phi_F + V_{CB}$ is the electron quasi-Fermi potential.

Substituting $\phi_S = 2\phi_F + V_{CB}$ into eqn (1) and solving for V_{CB}, we derive an expression for the pinch-off voltage V_P, defined as the value of V_{CB} for which the three-terminal MOS structure is in the upper limit of weak inversion:

$$V_P = \left(\sqrt{V_{GB} - V_{FB} + \frac{\gamma^2}{4} + \phi_t} - \frac{\gamma}{2}\right)^2 - 2\phi_F - \phi_t. \quad (2)$$

A slightly simplified version of eqn (2), presented in [1, p. 91], as V_{CBM}, and in Refs [11,16], is derived

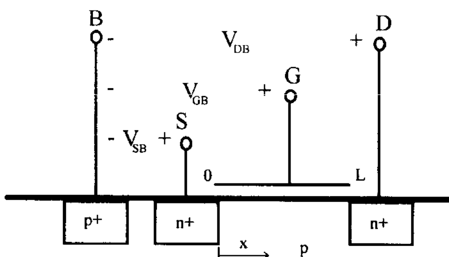

Fig. 1. Structure of an n-channel MOS transistor.

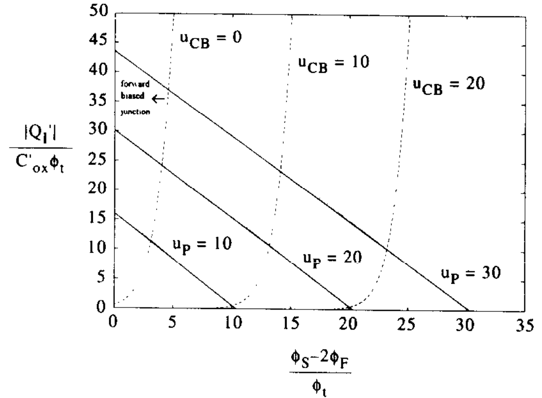

Fig. 2. Normalized inversion charge density vs normalized surface potential, computed from: (——) the linearized expression—eqn (4a); (····) and (– – – –) the theoretical implicit expression [1]—eqn (3a).

under the assumption that the inversion layer charge is negligible in the upper limit of weak inversion. If the thermal voltage terms are disregarded in eqn (2), the simplified expression of Refs [1,11,16] is obtained.

The main approximation in this work has been to consider the inversion (Q_I') and depletion (Q_B') charge densities as incrementally linear functions of ϕ_S for a constant gate-to-bulk voltage. According to the charge-sheet approximation, Q_I' and Q_B' are expressed as[1, p. 110]:

$$Q_I' = -C'_{ox}(V_{GB} - V_{FB} - \phi_S - \gamma\sqrt{\phi_S}) \quad (3a)$$

$$Q_B' = -C'_{ox}\gamma\sqrt{\phi_S}. \quad (3b)$$

Expanding eqns (3) in power series about $2\phi_F + V_P$ and disregarding the second and higher order terms we obtain, for constant V_{GB}:

$$Q_I' \cong C'_{ox}n[\phi_S - (2\phi_F + V_P)] + Q'_{IP} \quad (4a)$$

$$Q_B' \cong -C'_{ox}(n-1)[\phi_S - (2\phi_F + V_P)] + Q'_{BP} = -\frac{n-1}{n}(Q_I' - Q'_{IP}) + Q'_{BP} \quad (4b)$$

where the slope factor n[11,16] is the partial derivative of Q_I'/C'_{ox} with respect to ϕ_S for constant V_{GB}, calculated at pinch-off:

$$n = \left[\frac{1}{C'_{ox}}\frac{\partial Q_I'}{\partial \phi_S}\bigg|_{V_{GB}}\right]_{\phi_S = 2\phi_F + V_P} = 1 + \frac{\gamma}{2\sqrt{2\phi_F + V_P}} \quad (4c)$$

and Q'_{IP} and Q'_{BP} are the values of Q_I' and Q_B', respectively, at pinch-off (the first one according to the conventional weak inversion approximation):

$$Q'_{IP} = -(n-1)C'_{ox}\phi_t, \quad (4d)$$

$$Q'_{BP} = -C'_{ox}\gamma\sqrt{2\phi_F + V_P}. \quad (4e)$$

It should be pointed out that, unlike the conventional linearization about the source voltage, the linearization of Q_I' about the pinch-off channel voltage[11,16,17] preserves the symmetry of the

model with respect to drain and source. Figure 2 shows the dependence of Q_I' on ϕ_S. At constant V_{GB}, the linearization of Q_I' with respect to ϕ_S, according to eqn (4a), fits very well with the charge-sheet model, as can be noticed in Fig. 2. The fundamental approximations in eqns (4) have been applied throughout this work in order to obtain general expressions for the drain current and the total charges in terms of the inversion charge densities at the channel boundaries.

3. DRAIN CURRENT

In this section we formulate the drain current I_D as a very simple function of the inversion charge densities at the channel ends. According to [1, p. 109], I_D can be computed from:

$$I_D = \mu W\left(-Q_I'\frac{d\phi_S}{dx} + \phi_t\frac{dQ_I'}{dx}\right) \tag{5}$$

where the first term accounts for drift and the second for diffusion. From the approximated relationship between Q_I' and ϕ_S, eqn (4a), it follows that, for constant V_{GB}:

$$dQ_I' = nC_{ox}'\,d\phi_S. \tag{6}$$

The drain current can be evaluated by integrating eqn (5) along the channel length. The use of eqn (6) allows us to change the variable ϕ_S to Q_I' in expression (5), yielding:

$$I_D = -\frac{\mu}{nC_{ox}'}\frac{W}{L}\int_{Q_{IS}'}^{Q_{ID}'}(Q_I' - nC_{ox}'\phi_t)\,dQ_I' \tag{7}$$

where Q_{IS}' and Q_{ID}' are the inversion charge densities at source and drain, respectively. By means of the change of variable:

$$Q_{It}' = Q_I' - nC_{ox}'\phi_t, \tag{8a}$$

eqn (7) becomes:

$$I_D = -\frac{\mu}{nC_{ox}'}\frac{W}{L}\int_{Q_F'}^{Q_R'} Q_{It}'\,dQ_{It}'$$

$$= \frac{\mu W}{C_{ox}'L}\frac{(Q_F'^2 - Q_R'^2)}{2n} \tag{8b}$$

where Q_F' and Q_R' are the values of Q_{It}' evaluated at the source and drain ends, respectively.

A slight similarity can be observed between eqn (8b) and the formula of the drain current obtained in [7] from a linearization of $Q_I'(\phi_S)$ about the source voltage. Nevertheless, expression (8b) keeps the symmetry of the model with respect to source and drain.

4. TOTAL CHARGES

Here the total inversion (Q_I), source (Q_S), drain (Q_D) and depletion (Q_B) charges are evaluated as simple functions of the inversion charge densities at the source and drain ends. From our basic approximation in eqn (6) and from eqn (8a), eqn (5) can be rewritten as:

$$dx \cong -\frac{\mu W}{nC_{ox}'I_D}(Q_I' - nC_{ox}'\phi_t)\,dQ_I'$$

$$= -\frac{\mu W}{nC_{ox}'I_D}Q_{It}'\,dQ_{It}'. \tag{9}$$

Using eqns (8a) and (9) to change the variable of integration from x to Q_{It}' in the definition of Q_I [1, p. 252], it follows that:

$$Q_I = W\int_0^L Q_I'\,dx = -\frac{\mu W^2}{I_D nC_{ox}'}$$

$$\times\left[\int_{Q_F'}^{Q_R'} Q_{It}'^2\,dQ_{It}' + nC_{ox}'\phi_t\int_{Q_F'}^{Q_R'} Q_{It}'\,dQ_{It}'\right]. \tag{10}$$

Using eqn (8b) we easily derive the expression of Q_I reported in Table 2.

The integration of eqn (9) from the source to an arbitrary point of the channel leads to:

$$x = \frac{\mu W}{nC_{ox}'}\frac{(Q_F'^2 - Q_{It}'^2)}{2I_D}. \tag{11}$$

Using eqns (9), (8a) and (11) into the integral defining Q_D [1, p. 259] allows changing the variable of integration, resulting in

$$Q_D = W\int_0^L \frac{x}{L}Q_I'\,dx = -\frac{\mu^2 W^3}{2n^2C_{ox}'^2 L I_D^2}$$

$$\times\int_{Q_F'}^{Q_R'}(Q_F'^2 - Q_{It}'^2)(Q_{It}'^2 + nC_{ox}'\phi_t Q_{It}')\,dQ_{It}'. \tag{12}$$

After integration, eqn (12) gives the expression of Q_D reported in Table 2. Taking into account the symmetry of the MOSFET, it follows that: $Q_S = Q_I - Q_D$.

Finally, using eqns (4b), (8a) and (9) to perform a

Table 1. Auxiliary functions and parameters

Quantity	Expression
Q_F'	$Q_I'(V_{SB}, V_{GB}) - nC_{ox}'\phi_t$
Q_R'	$Q_I'(V_{DB}, V_{GB}) - nC_{ox}'\phi_t$
D_F'	$D'(V_{SB}, V_{GB})$
D_R'	$D'(V_{DB}, V_{GB})$
A	$\frac{2}{3}WL$
B	$\frac{\mu W}{C_{ox}'L}$

$D'(V_{CB}, V_{GB})$ is the derivative of Q_I' with respect to V_C at constant V_G.

Table 2. Drain current, total charges and small signal parameters

Quantity	Expression
Q_I	$WL\left[\frac{2}{3}\frac{Q_F'^2+Q_F'Q_R'+Q_R'^2}{Q_F'+Q_R'}+nC_{ox}'\phi_t\right]$
Q_S	$WL\left[\frac{6Q_F'^3+12Q_R'Q_F'^2+8Q_R'^2Q_F'+4Q_R'^3}{15(Q_F'+Q_R')^2}+\frac{n}{2}C_{ox}'\phi_t\right]$
I_D	$B\frac{(Q_F'^2-Q_R'^2)}{2n}$
g_{mS}	$-\frac{B}{n}Q_F'D_F'$
C_{gs}	$\frac{A}{n}\left[1-\frac{Q_R'^2}{(Q_F'+Q_R')^2}\right]D_F'$
C_{bs}	$(n-1)C_{gs}$
C_{gb}	$\frac{n-1}{n}(C_{ox}-C_{gs}-C_{gd})$
C_{ss}	$-\frac{2}{15}\frac{WL}{(Q_F'+Q_R')^3}(3Q_F'^3+9Q_R'Q_F'^2+8Q_R'^2Q_F')D_F'$
C_{sg}	$-\frac{(C_{ss}+C_{sd})}{n}$
Q_B	$-WLC_{ox}'\left[\frac{(n-1)^2}{n}\phi_t+\frac{\gamma^2}{2(n-1)}\right]-\frac{n-1}{n}Q_I$
Q_D	Q_I-Q_S
g_{mG}	$\frac{g_{mS}-g_{mD}}{n}$
g_{mD}	$-\frac{B}{n}Q_R'D_R'$
C_{gd}	$\frac{A}{n}\left[1-\frac{Q_F'^2}{(Q_F'+Q_R')^2}\right]D_R'$
C_{bd}	$(n-1)C_{gd}$
C_{bg}	C_{gb}
C_{sd}	$-\frac{4}{15}\frac{WL}{(Q_F'+Q_R')^3}(Q_R'^3+3Q_F'Q_R'^2+Q_F'^2Q_R')D_R'$
C_{sb}	$(n-1)C_{sg}$

change of variable in the the integral defining Q_B[1, p. 252], we obtain

$$Q_B = W\int_0^L Q_B'\,dx = \frac{\mu W^2}{nC_{ox}'I_D}$$
$$\times\left[\frac{n-1}{n}\int_{Q_F'}^{Q_R'}(Q_{It}'^2+Q_{It}'nC_{ox}'\phi_t)\,dQ_{It}' - \left(Q_{BP}'+\frac{n-1}{n}Q_{IP}'\right)\int_{Q_{IS}}^{Q_{ID}}Q_{It}'\,dQ_{It}'\right] \quad (13)$$

where the first integral is proportional to the inversion charge and the second one is proportional to the drain current. Thus, eqn (13) leads directly to:

$$Q_B = \frac{n-1}{n}(Q_{IP}'WL - Q_I) + Q_{BP}'WL. \quad (14)$$

The set of expressions previously derived for the drain current and total charges is the basis for a MOSFET electrical model expressed in terms of the inversion charge densities at the source and drain boundaries.

5. EXPLICIT FORMULATION OF THE INVERSION CHARGE DENSITY

In this section we present an explicit and accurate expression for the inversion charge density. We have first derived an integral expression for Q_I' based only on our basic approximation, eqns (4). Afterwards, we have applied the approximation of the semiconductor capacitance developed in Appendix C to the integral expression for Q_I'.

By expressing $Q_I'(\phi_S)$ as in eqn (3a), we remark that:

$$\left.\frac{\partial Q_I'}{\partial V_{CB}}\right|_{V_{GB}} = \left.\frac{\partial Q_I'}{\partial \phi_S}\right|_{V_{GB}}\left.\frac{\partial \phi_S}{\partial V_{CB}}\right|_{V_{GB}}. \quad (15)$$

The first derivative in the right-hand side of eqn (15) can be calculated from the linear approximation of $Q_I'(\phi_S)$, eqn (4a); the second one can be evaluated by exactly differentiating eqn (1) with respect to V_{CB}:

$$\left.\frac{\partial \phi_S}{\partial V_{CB}}\right|_{V_{GB}} = \frac{\dfrac{\gamma\, e^{(\phi_S-2\phi_F-V_{CB})/\phi_t}}{2\sqrt{\phi_S+\phi_t\, e^{(\phi_S-2\phi_F-V_{CB})/\phi_t}}}}{1+\dfrac{\gamma[1+e^{(\phi_S-2\phi_F-V_{CB})/\phi_t}]}{2\sqrt{\phi_S+\phi_t\, e^{(\phi_S-2\phi_F-V_{CB})/\phi_t}}}}. \quad (16)$$

Using the definitions of the inversion (C_i') and semiconductor (C_c') capacitances per unit area, presented in [1, p. 80], valid for the inversion region, eqn (16) is compactly rewritten in the form:

$$\left.\frac{\partial \phi_S}{\partial V_{CB}}\right|_{V_{GB}} = \frac{C_i'/C_{ox}'}{1+C_c'/C_{ox}'}. \quad (17)$$

Substituting eqn (17) into eqn (15) and applying our basic approximation of eqn (6), we obtain:

$$\left.\frac{\partial Q_{\mathrm{I}}'}{\partial V_{\mathrm{CB}}}\right|_{V_{\mathrm{GB}}} = n\frac{C_{\mathrm{i}}'}{1 + C_{\mathrm{c}}'/C_{\mathrm{ox}}'}. \quad (18a)$$

Hence, the inversion charge density can be determined from:

$$Q_{\mathrm{I}}' = Q_{\mathrm{IP}}' + \int_{V_{\mathrm{P}}}^{V_{\mathrm{CB}}} n\frac{C_{\mathrm{i}}'}{1 + C_{\mathrm{c}}'/C_{\mathrm{ox}}'}\,\mathrm{d}V_{\mathrm{CB}}. \quad (18b)$$

In strong inversion (including moderate inversion) we use the following relationship derived in Appendix C:

$$C_{\mathrm{c}}' \cong C_{\mathrm{i}}' \cong C_{\mathrm{ox}}' n\frac{(V_{\mathrm{P}} - V_{\mathrm{CB}})}{2\phi_{\mathrm{t}}} + (n-1)C_{\mathrm{ox}}' \quad \text{for } V_{\mathrm{CB}} \leqslant V_{\mathrm{P}}. \quad (19)$$

This approximation for C_{i}' is such that the physical property $C_{\mathrm{i}}' = C_{\mathrm{b}}'$ is verified in the transition from weak to strong inversion[1, p. 80]. Substituting eqn (19) into eqn (18b), we find that:

$$Q_{\mathrm{I}}' = -C_{\mathrm{ox}}'\left[n(V_{\mathrm{P}} - V_{\mathrm{CB}}) - 2\phi_{\mathrm{t}}\ln\left(1 + \frac{V_{\mathrm{P}} - V_{\mathrm{CB}}}{2\phi_{\mathrm{t}}}\right) + (n-1)\phi_{\mathrm{t}}\right] \quad \text{for } V_{\mathrm{CB}} \leqslant V_{\mathrm{P}}. \quad (20a)$$

For weak inversion, we have adopted here the conventional expression of the inversion charge density[1,11,16]:

$$Q_{\mathrm{I}}' = -C_{\mathrm{ox}}'(n-1)\phi_{\mathrm{t}}\,\mathrm{e}^{(V_{\mathrm{P}} - V_{\mathrm{CB}})/\phi_{\mathrm{t}}} \quad \text{for } V_{\mathrm{CB}} \geqslant V_{\mathrm{P}}. \quad (20b)$$

Equations (20) provide a continuous transition from weak to strong inversion as well as from conduction to saturation for Q_{I}' and its first order partial derivatives with respect to V_{GB} and V_{CB}. The approximation obtained for the inversion charge density in strong inversion differs from the conventional linear approximation[11,16], mainly by the logarithmic term. As illustrated in Fig. 3, this term improves the precision of the inversion charge density, especially in the so-called moderate inversion region.

Finally, in order to provide more physical insight

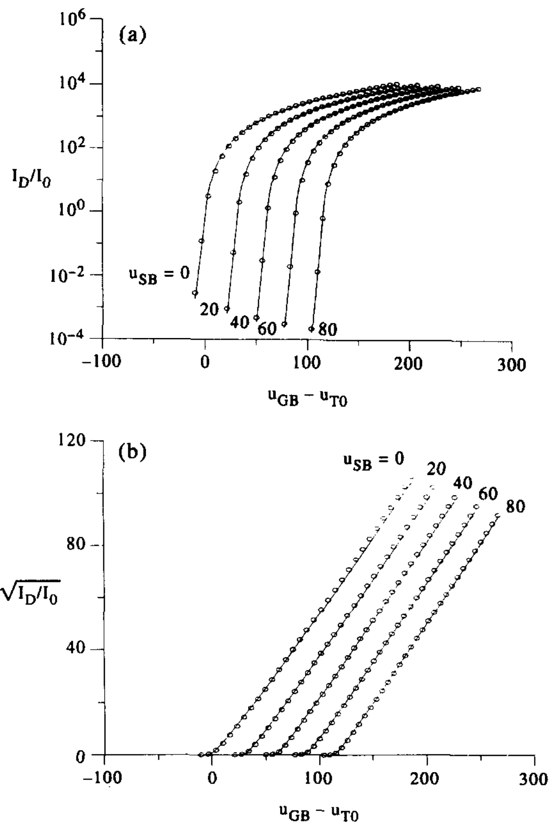

Fig. 4. (a) Normalized drain current in saturation vs normalized gate voltage and (b) square root of normalized drain current in saturation vs normalized gate voltage, computed from: (——) our model—eqns (8) and (20); (○○○○) the charge-sheet model[1,5].

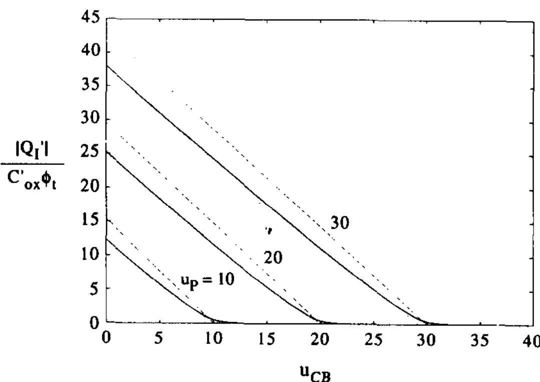

Fig. 3. Normalized inversion charge density vs normalized channel voltage computed from: (——) our model—eqns (20); (····) the theoretical implicit expression[1]—eqns (3a) and (1); (– – – –) the linear expression with respect to V_{CB}: $|Q_{\mathrm{I}}'| = n(V_{\mathrm{P}} - V_{\mathrm{CB}})$[11,16].

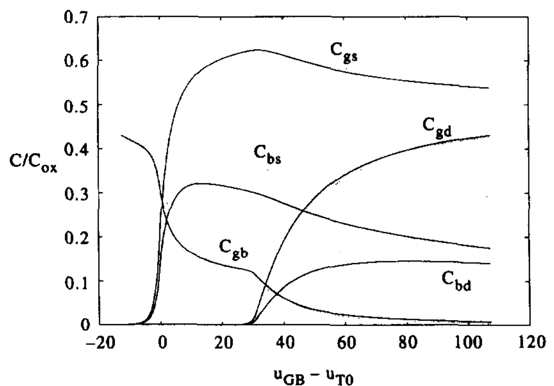

Fig. 5. Normalized intrinsic small-signal capacitances vs normalized gate-to-source voltage, for $u_{\mathrm{SB}} = 0$ and $u_{\mathrm{DB}} = 20$, computed from: (——) our model—Table 2 and eqns (20); (····) the charge sheet model[1,6].

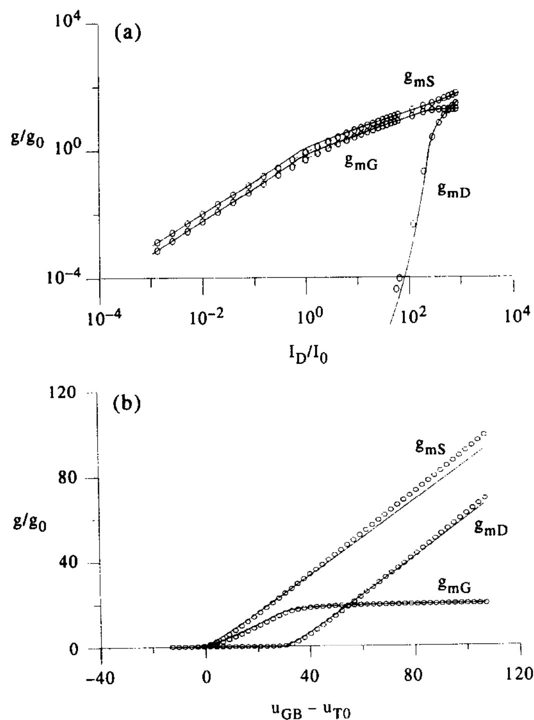

Fig. 6. Normalized small-signal transconductances vs normalized drain current, for $u_{SB} = 0$ and $u_{DB} = 20$, computed from: (——) our model—Table 2 and eqns (20); (· · · ·) our model—eqns (A9) and (20); (○ ○ ○ ○) the charge sheet model[1,6].

in our model let us extend our approximation to the surface potential. Equation (4a) can be rewritten as:

$$\phi_S = 2\phi_F + V_P + \frac{Q'_I - Q'_{IP}}{nC'_{ox}}. \quad (21)$$

The substitution of the strong (including moderate) inversion approximation of Q'_I from eqn (20a) into eqn (21) leads to:

$$\phi_S = 2\phi_F + V_{CB} + \frac{2\phi_t}{n}\ln\left(1 + \frac{V_P - V_{CB}}{2\phi_t}\right) \quad \text{for } V_{CB} \leqslant V_P, \quad (22a)$$

which is continuous with the conventional weak inversion approximation:

$$\phi_S = 2\phi_F + V_P \quad \text{for } V_{CB} \geqslant V_P. \quad (22b)$$

Note that our model includes a logarithmic term that gives a slight variation of ϕ_S with V_{GB} in strong inversion, improving the conventional approximation $(2\phi_F + V_{CB})$ in this region of operation.

6. SIMULATION RESULTS

Figure 4 shows the drain current of a long-channel NMOS transistor in saturation computed from our model and from the Brews' charge-sheet model[1,5]. In Fig. 6 the small-signal transconductances computed from our model are compared to those calculated from the Brews' model. Agreement with charge-sheet theory is excellent. Figure 5 illustrates the capacitances C_{gs}, C_{bs}, C_{gd}, C_{bd} and C_{gb}, calculated from our expressions and according to [6]. The results for the gate capacitances are very good. The errors in the bulk capacitances exhibit maximum values deep in strong inversion owing to the linear approximation of the depletion charge density, eqn (4b). The maximum errors verified in the bulk capacitances are less than $0.15C_{ox}$ and do not affect meaningfully the behavior of most circuits since, according to [1, p. 318], these capacitances are generally in parallel with larger capacitances or even short-circuited (C_{bs}).

7. CONCLUSIONS

We have accomplished a general explicit MOSFET model (Tables 1 and 2) that uses the inversion charge density as the key variable. A smooth variation of the device characteristics, including small signal parameters, is guaranteed through the entire inversion region. Only the customary MOSFET parameters have been employed in our model.

Short and narrow channel effects can be modeled as in Ref. [17], where the pinch-off voltage V_P is a function of both the channel length and width. Also field-dependent mobility can be included in the usual way[1, p. 141].

REFERENCES

1. Y. P. Tsividis, *Operation and Modeling of the MOS Transistor*. McGraw-Hill, New York (1987).
2. R. C.-H. Chang and B. J. Sheu, in *Proc. IEEE Int. Symp. on Circ. and Syst.*, London, U.K., pp. 311–314 (1994).
3. N. D. Arora, R. Rios, C.-L. Huang and K. Raol, *IEEE Trans. Electron Dev.* **ED-41,** 988 (1994).
4. Y. Tsividis and G. Masetti, *IEEE Trans. CAD* **CAD-3,** 72 (1984).
5. J. R. Brews, *Solid-St. Electron.* **21,** 345 (1978).
6. C. Turchetti, G. Masetti and Y. Tsividis, *Solid-St. Electron.* **26,** 941 (1983).
7. M. Bagheri and Y. Tsividis, *IEEE Trans. Electron. Dev.* **ED-32,** 2383 (1985).
8. M. Miura-Mattausch, *IEEE Trans. CAD* **CAD-13,** 610 (1994).
9. A. R. Boothroyd, S. W. Tarasewicz and C. Slaby, *IEEE Trans. CAD* **CAD-10,** 1512 (1991).
10. C. Turchetti and G. Masetti, *IEEE Trans. CAD* **CAD-3,** 117 (1984).
11. C. Enz, High-precision CMOS micropower amplifiers. Ph.D. Thesis No 802. EPF-Lausanne (1989).
12. B. Iñiguez and E. G. Moreno, *Electron. Lett.* **29,** 1036 (1993).
13. C. K. Park, C. Y. Lee, K. Lee, B. J. Moon, Y. H. Byun and M. Shur, *IEEE Trans. Electron. Dev.* **ED-38,** 399 (1991).
14. M. Shur, T. A. Fjeldly, T. Ytterdal and K. Lee, *Solid-St. Electron.* **35,** 1795 (1992).
15. A. T. Behr, M. C. Schneider, S. Noceti Filho and C. G. Montoro, *IEEE J. Solid-St. Circuits* **SC-27,** 1470 (1992).
16. E. A. Vittoz, *Intensive Summer Course on CMOS VLSI Design—Analog & Digital*. EPF, Lausanne (1989).

17. C. C. Enz, F. Krummenacher and E. A. Vittoz, to be published in *Analog Integrated Circuits Signal Process.* (1995).

APPENDIX A

Small Signal Parameters

The MOSFET intrinsic capacitances for quasi-static operation are defined[1, p. 355] by the general expressions:

$$C_{kj} = -\left.\frac{\partial Q_K}{\partial V_J}\right|_0 \quad k \neq j \tag{A1a}$$

$$C_{jj} = \left.\frac{\partial Q_J}{\partial V_J}\right|_0 \tag{A1b}$$

where Q_K and Q_J are any of the charges Q_S, Q_D, Q_B or Q_G and V_J is any of the gate (V_G), source (V_S), drain (V_D) or bulk (V_B) voltages. The notation "0" indicates that the derivatives are evaluated at the bias point. According to [1, p. 358], a complete quasi-static model of capacitances is performed by calculating only nine independent capacitances.

The total gate charge is given by:

$$Q_G = -Q_B - Q_I - Q_0, \tag{A2}$$

where Q_0 is the effective interface charge, assumed to be independent of the terminal voltages. Substituting eqn (14) into eqn (A2), we obtain:

$$Q_G = -Q_P - \frac{Q_I}{n} - Q_0 \tag{A3a}$$

where

$$Q_P = Q'_{BP}WL + \frac{n-1}{n}Q'_{IP}WL. \tag{A3b}$$

From the expressions of Q_I and Q_S in Table 2 and from eqns (A1), (A3a) and (8a), we find the expressions for C_{gs}, C_{gd}, C_{sd} and C_{ss} shown in Table 2.

From eqns (A1a), (14) and (A3a), it follows that:

$$C_{bs} = (n-1)C_{gs} \tag{A4a}$$

$$C_{bd} = (n-1)C_{gd}. \tag{A4b}$$

Differentiating eqn (2) with respect to V_G and V_B and comparing to eqn (4c), we find that[16]

$$\left.\frac{\partial V_P}{\partial V_G}\right|_{V_B} = -\left.\frac{\partial V_P}{\partial V_B}\right|_{V_G} \cong \frac{1}{n}. \tag{A5}$$

From eqn (A3b), (4d), (4e) and (A5) we obtain:

$$\left.\frac{\partial Q_P}{\partial V_G}\right|_{V_B} = -\left.\frac{\partial Q_P}{\partial V_B}\right|_{V_G} = -\frac{n-1}{n}C_{ox} \times\left[1-\frac{1}{2}\left(\frac{\phi_t}{2\phi_F+V_P}\right)\left(1-\frac{1}{n^2}\right)\right] \tag{A6a}$$

where $C_{ox} = WLC'_{ox}$.

In eqn (A6a), since $\phi_t \ll 2\phi_F + V_P$, the second term between brackets is negligible compared to unity. Hence, we can rewrite eqn (A6a) as:

$$\left.\frac{\partial Q_P}{\partial V_G}\right|_{V_B} = -\left.\frac{\partial Q_P}{\partial V_B}\right|_{V_G} = -\frac{n-1}{n}C_{ox}. \tag{A6b}$$

Equation (A6b) could be readily obtained if we had neglected the variation of n with V_G or V_B in expressions (A3b) and (4d). In the remaining demonstrations of this Appendix, where necessary, the derivatives of n with respect to V_G or V_B are neglected. Such an approximation is also assumed elsewhere[1, p. 316] and [11,17].

Taking into account the relationships between $\partial Q'_I/\partial V_G$ and $\partial Q'_I/\partial V_C$ stated by eqn (B2b) and between $\partial Q'_I/\partial V_B$ and $\partial Q'_I/\partial V_C$ stated by eqn (B3b), in Appendix B, we have from the expressions of Q_I, C_{gs} and C_{gd} in Table 2 and from eqn (8a):

$$\left.\frac{\partial Q_I}{\partial V_G}\right|_{V_S,V_D,V_B} = -(C_{gs}+C_{gd}) \tag{A7a}$$

$$\left.\frac{\partial Q_I}{\partial V_B}\right|_{V_S,V_D,V_G} = -(n-1)(C_{gs}+C_{gd}). \tag{A7b}$$

Hence, from eqns (A1a), (14), (A3a), (A6b) and (A7), we obtain the expressions of C_{gb} and C_{bg} in Table 2.

Finally, from the expressions of Q_S, C_{ss} and C_{sd} in Table 2 and from eqns (A1a), (8a) and (B2b), the expression of C_{sg} in Table 2 follows. Applying the relationships of eqns (B2b) and (B3b) we also determine the expression of C_{sb} in Table 2.

The MOSFET source, drain and gate transconductances[11,16] are calculated using eqns (8) and are shown in Table 2. g_{mG} has been derived by applying the relationship between $\partial Q'_I/\partial V_G$ and $\partial Q'_I/\partial V_C$ described by eqn (B2b).

Instead of differentiating the expression proposed for I_D, eqn (8b), we can adopt the alternative expression[1, p. 120]:

$$I_D = \mu\frac{W}{L}\int_{V_{SB}}^{V_{DB}}(-Q'_I)\,dV_{CB}. \tag{A8}$$

Hence, the transconductances become:

$$g_{mS} = -\mu\frac{W}{L}Q'_{IS} \tag{A9a}$$

$$g_{mD} = -\mu\frac{W}{L}Q'_{ID} \tag{A9b}$$

$$g_{mG} = -\mu\frac{W}{L}\int_{V_{SB}}^{V_{DB}}\frac{\partial Q'_I}{\partial V_{GB}}\,dV_{CB} = \frac{g_{mS}-g_{mD}}{n}. \tag{A9c}$$

It is noticeable that while the set of expressions for the transconductances in Table 2 is affected by the approximations employed to compute the drain current, eqns (A9a) and (A9b) are extremely accurate. Hence, as observed from Fig. 6(a), the latter set of expressions improves the accuracy of the model in the moderate inversion region.

APPENDIX B

Derivatives of the Inversion Charge Density

Through the application of the linear approximation of $Q'_I(\phi_S)$ presented in Section 2, we have derived important relationships between the partial derivatives of Q'_I with respect to V_{CB}, the gate-to-bulk voltage V_{GB} and the bulk potential V_B.

According to [1, p. 69]:

$$\left.\frac{\partial Q'_I}{\partial V_{GB}}\right|_{V_{CB}} = -\frac{C'_i}{1+C'_c/C'_{ox}}. \tag{B1}$$

The comparison between eqns (15), (17) and (B1) leads to the general relationship:

$$\left.\frac{\partial Q'_I}{\partial V_{GB}}\right|_{V_{CB}} = -C'_{ox}\frac{\left.\dfrac{\partial Q'_I}{\partial V_{CB}}\right|_{V_{GB}}}{\left.\dfrac{\partial Q'_I}{\partial \phi_S}\right|_{V_{GB}}}, \tag{B2a}$$

which can be simplified through the use of the basic approximation of eqn (6):

$$\left.\frac{\partial Q'_I}{\partial V_G}\right|_{V_C,V_B} \cong -\frac{1}{n}\left.\frac{\partial Q'_I}{\partial V_C}\right|_{V_G,V_B}. \tag{B2b}$$

The derivative of Q'_I with respect to V_B can be written as:

$$\left.\frac{\partial Q'_I}{\partial V_B}\right|_{V_C,V_G} = \left.\frac{\partial Q'_I}{\partial V_{GB}}\right|_{V_{CB}}\left.\frac{\partial V_{GB}}{\partial V_B}\right|_{V_G} + \left.\frac{\partial Q'_I}{\partial V_{CB}}\right|_{V_{GB}}\left.\frac{\partial V_{CB}}{\partial V_B}\right|_{V_G}. \tag{B3a}$$

Since $\partial V_{GB}/\partial V_B = \partial V_{CB}/\partial V_B = -1$, applying the property stated by eqn (B2b), we find that:

$$\left.\frac{\partial Q'_I}{\partial V_B}\right|_{V_C,V_G} \cong -\frac{(n-1)}{n}\left.\frac{\partial Q'_I}{\partial V_C}\right|_{V_G,V_B} = (n-1)\left.\frac{\partial Q'_I}{\partial V_G}\right|_{V_C,V_B}. \quad \text{(B3b)}$$

APPENDIX C

Approximation of the Semiconductor Capacitance

The semiconductor capacitance per unit area is usually split into two components, the inversion and depletion capacitances[1, p. 80].

Expressing the semiconductor charge density in inversion as[1]:

$$Q'_C = -C'_{ox}\gamma\sqrt{\phi_S + \phi_t e^{(\phi_S - 2\phi_F - V_{CB})/\phi_t}}, \quad \text{(C1)}$$

it follows immediately from the expression of the depletion capacitance in [1, p. 80], that:

$$C'_b = \frac{\gamma^2 C'^2_{ox}}{2|Q'_C|}. \quad \text{(C2a)}$$

Adopting for Q'_B the charge-sheet approximation of eqn (3b), the expression of C'_i in [1, p. 80], can be rewritten in the compact form:

$$C'_i = \frac{Q'^2_C - Q'^2_B}{2\phi_t|Q'_C|}. \quad \text{(C2b)}$$

Since $Q'_I = Q'_C - Q'_B$[1,4], eqn (C2b) is equivalent to:

$$C'_i = \frac{|Q'_I|}{2\phi_t}\left(1 + \frac{Q'_B}{Q'_C}\right). \quad \text{(C3)}$$

In strong inversion, we assume that the inversion component of C'_c is much greater than the depletion component, so that:

$$C'_c \cong C'_i. \quad \text{(C4)}$$

In this region of operation, the surface potential ϕ_S approaches the value $2\phi_F + V_{CB}$. Substituting this approximation into the linear expression of Q'_I, eqn (4a), and applying it to eqn (C3), we approximate the inversion capacitance in strong inversion, including the so-called moderate inversion region, to:

$$C'_i = \frac{C'_{ox}}{2\phi_t}n(V_P - V_{CB})\left(1 + \frac{Q'_B}{Q'_C}\right) - \frac{Q'_{IP}}{2\phi_t}\left(1 + \frac{Q'_B}{Q'_C}\right)$$
$$\text{for } V_{CB} \leqslant V_P. \quad \text{(C5)}$$

The first term in the right-hand side of eqn (C5) prevails deep in strong inversion (for high values of V_{GB}), where $Q'_B \ll Q'_C$; hence, in this term $(1 + Q'_B/Q'_C)$ can be approximated to 1. The second term of eqn (C5) prevails near threshold, where $Q'_B \cong Q'_C$, such that in this second term $(1 + Q'_B/Q'_C)$ can be better approximated to 2. Taking into account these two approximations and eqn (C4) we obtain eqn (19), which is a slight modification of the semiconductor capacitance model used in [15] to determine the harmonic distortion in MOS gate capacitors in strong inversion. The term $(n-1)C'_{ox}$ guarantees continuity between eqn (19) and the classical approximation of the semiconductor capacitance in weak inversion:

$$C'_c \cong C'_b \cong \frac{\gamma}{2\sqrt{2\phi_F + V_P}}C'_{ox} = (n-1)C'_{ox}$$
$$\text{for } V_{CB} \geqslant V_P. \quad \text{(C6)}$$

APPENDIX D

Definitions and Technological Parameters

$$u_{GB} = \frac{V_{GB}}{\phi_t} \quad u_{CB} = \frac{V_{CB}}{\phi_t} \quad u_{SB} = \frac{V_{SB}}{\phi_t} \quad u_{DB} = \frac{V_{DB}}{\phi_t}$$

$$u_{FB} = \frac{V_{FB}}{\phi_t} \quad u_P = \frac{V_P}{\phi_t} \quad u_{T0} = \frac{V_{T0}}{\phi_t}$$

$$I_0 = \frac{\mu W}{L}C'_{ox}\phi_t^2 \quad g_0 = \frac{\mu W}{L}C'_{ox}\phi_t$$

$N_A = 5 \times 10^{15}\,\text{cm}^{-3}$ $\quad t_{ox} = 878$ Å $\quad V_{FB} = -1.18$ V.